Development and Execution of a Production-Scale Continuous [2 + 2] Photocycloaddition

Matthew G. Beaver,* En-xuan Zhang,* Zhi-qing Liu, Song-yuan Zheng, Bin Wang, Jiang-ping Lu, Jian Tao, Miguel Gonzalez, Siân Jones, and Jason S. Tedrow

Cite This: https://dx.doi.org/10.1021/acs.oprd.0c00185

Read Online

ACCESS | Metrics & More | Article Recommendations | Supporting Information

ABSTRACT: This article details the approach to large-scale production of cyclobutane **2** by the continuous-flow [2 + 2] photocycloaddition of maleic anhydride and ethylene, including (1) focused reaction optimization and development of a robust isolation protocol, (2) the approach to equipment design and process safety, and (3) the results of commissioning tests and production runs delivering the target compound at throughputs exceeding 5 kg/day.

KEYWORDS: photochemistry, photocycloaddition, continuous manufacturing, flow chemistry

■ INTRODUCTION

Continued advances in the intensity and availability of light-emitting diodes (LEDs) have facilitated the development of a wealth of novel photochemical transformations for application in organic synthesis.[1] Despite the potential for these processes to benefit the large-scale production of active pharmaceutical ingredients (APIs), implementation of light-mediated processes at manufacturing scale (>100 kg) remains elusive because of the poor penetration of light through traditional batch reactors. Continuous manufacturing (i.e., flow chemistry) has proven to address this physical deficiency by transfer of the reaction stream through a plug-flow reactor (PFR)[2] or continuously stirred tank reactor (CSTR)[3] placed in close proximity to a high-intensity light source.[4]

A recent program required the large-scale production of cyclobutane **2**. A one-step synthesis of the target compound was proposed utilizing the [2 + 2] photocycloaddition of the inexpensive and readily available reagents maleic anhydride (**1**) and ethylene (Scheme 1).[5] Recent literature precedent has

Scheme 1. [2 + 2] Photocycloaddition to Prepare Cyclobutane 2

maleic anhydride (**1**) → cyclobutane **2**

ethylene (gas), light source, photosensitizer, solvent, temp

since corroborated this approach by continuous operation of a PFR,[6,7] but the challenge remains translation from lab-scale equipment (g/day) to the production setting (kg/day), as maleic anhydride has proven incredibly inefficient in photochemical processes compared with its substituted derivatives and maleimide congeners.[7,8] Described herein are the development and execution of a high-throughput (>5 kg/

day) photochemical flow process and corresponding batch isolation to generate >250 kg quantities of cyclobutane **2** as a crystalline solid meeting the target purity profile.
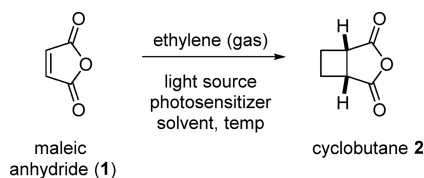
■ RESULTS AND DISCUSSION

A multistage approach was advanced to support the development and execution of a production-scale process to prepare cyclobutane **2**: (1) focused reaction optimization; (2) proof of concept through intermediate scale-up (ca. 500 g/day) and development of a robust isolation protocol; and (3) equipment design, safety assessment, and execution of the production-scale process to prepare >5 kg/day of the target compound **2**.

Optimization of the Reaction Parameters. Internal optimization efforts and parallel advances disclosed in the photochemical literature highlighted the dramatic efficiency gains using LEDs as a light source for the target transformation (Scheme 1) compared with a medium-pressure Hg lamp.[5] Similarly, benzophenone was identified as the optimal photosensitizer for this process, as corroborated by recent literature reports.[6,7] All of the optimizations described herein utilized 365 nm LEDs as the light source in combination with benzophenone as the photosensitizer.

An evaluation of solvents identified acetone as optimal in terms of balancing reaction conversion, efficiency, and purity profile. In these experiments, a 0.25 M solution of **1**[9] containing benzophenone (10 mol %) was sparged with ethylene at ambient pressure and recirculated through 0.31 L of fluorinated ethylene propylene (FEP) tubing[10] (o.d. = 3 mm, i.d. = 2 mm) wrapped around 365 nm LEDs (0.25 L
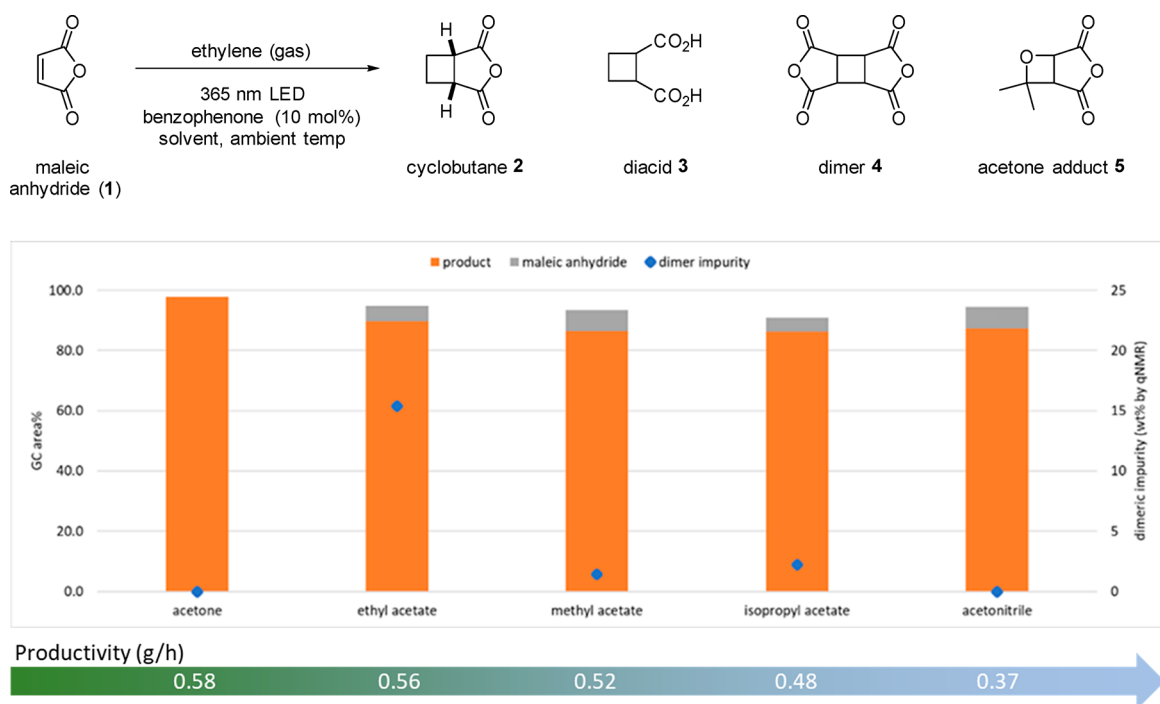
A

Figure 1. Effect of the solvent choice on the reaction conversion and purity profile.

irradiation volume) until <10% of the starting material remained as determined by gas chromatography (GC) area %.[11] A representative summary of this optimization effort is depicted in Figure 1, where a range of solvents are shown to provide comparable efficiencies for the desired transformation. The diacid impurity 3 could be well-controlled (<1 GC area %) through use of anhydrous solvents and exclusion of water in the isolation process. Ultimately, the differentiating factor for solvent choice arose from an evaluation of the ¹H NMR spectra of the crude reaction streams; specifically, the dimer impurity 4, which was not detectable by the GC method, was present at elevated levels for all of the ester solvents evaluated.[12] The isolated impurity demonstrated poor solubility in the range of solvents evaluated and was deemed a clogging risk for extended continuous operation (ca. weeks). For this reason, acetone was chosen for all subsequent optimization experiments and demonstration runs. The Paternó–Büchi adduct of acetone and maleic anhydride (5), the major product formed upon irradiation with a medium-pressure Hg lamp,[13] was not observed under these conditions.

The impact of pressure and temperature on the solubility of ethylene in acetone was evaluated experimentally to support the reactor design (Figure 2). The pressure range investigated was guided by the maximum allowable rating of the tubing anticipated for use in the production setting: ~10 bar (25 °C) for 10 mm o.d. FEP tubing with a 1 mm wall thickness. A target pressure of 6–8 bar was selected to provide an appreciable safety margin during operation. As has been reported previously for ethylene in organic solvents,[6,14] a decrease in temperature was associated with the expected increase in ethylene solubility. Despite this solubility improvement, existing precedent demonstrated a negligible correlation between reaction efficiency and temperature;[7] therefore, the decision was made to pursue operation at 20 °C to minimize complexity in reactor design.
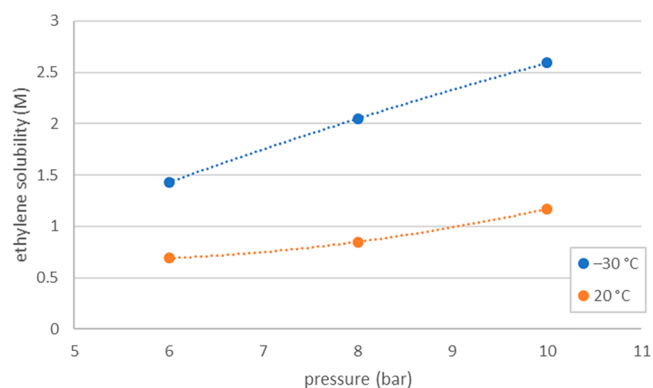

Figure 2. Effect of temperature and pressure on the solubility of ethylene in acetone.

An evaluation of the photosensitizer loading demonstrated a positive correlation with the reaction efficiency but a negative impact on the crystallization efficiency and overall process yield. The benzophenone loading study was performed in a similar manner to the aforementioned solvent screen: 0.25 M solutions of 1 in acetone containing various loadings of benzophenone were sparged with ethylene and recirculated through FEP tubing wrapped around 365 nm LEDs until <5% of the starting material remained as determined by GC area %. A background reaction was performed in the absence of photosensitizer, which provided 40 GC area % cyclobutane 2 after 51 h of irradiation and a corresponding productivity of 0.13 g/h (Table 1, entry 1). Increasing the loading in 5 mol % increments resulted in the expected improvement in the reaction efficiency; however, increasing levels of benzophenone negatively impacted the product purity upon crystallization.[15] A benzophenone loading of 10 mol % was chosen to balance the reaction and crystallization efficiencies. Details of the isolation optimization are provided in a subsequent section.

Table 1. Effect of the Photosensitizer Loading on the Reaction Productivity

entry	benzophenone loading (mol %)	reaction productivity (g/h)
1	0	0.13
2	5	0.55
3	10	0.58
4	15	0.70
5	20	0.77

With an understanding of the factors that influence the chemical efficiency, the focus shifted to an evaluation of the equipment required to support the 500 g/day proof-of-concept run. Considerations were made to facilitate direct translation to the production setting, and the following parameters were investigated: tubing diameter, gas–liquid mixing, and light intensity (Table 2). The volumetric throughputs estimated for production required significantly larger tubing than typically employed for lab-scale photochemical reactions (ca. 1–2 mm i.d.). Using the high-power light sources detailed in Table 2, o.d. tubing sizes of 6 and 10 mm provided comparable productivities under identical reaction conditions (Table 2, entries 1 and 2). The mode of gas–liquid mixing was also evaluated at the increased flow rates and tubing diameters, demonstrating that a union tee mixer and mixing tank (residence time = 1 min) provided comparable efficiencies (Table 2, entries 3 and 4). The tee mixer was employed for the 500 g/day demonstration but replaced by a mixing tank with a residence time of 30 min at production scale to eliminate ethylene slugs observed at the increased flow rates. Finally, an evaluation of the reaction productivity versus the light source intensity demonstrated a nearly linear correlation over the conditions examined, consistent with a photon-limited process (Table 2, entries 5–7).

Demonstration Run Targeting 500 g/day Throughput. The flow system with 10 mm o.d. FEP tubing and 3 × 300 W surface-mounted LED panels (irradiation intensity at tubing = 60 mW/cm^2) was installed, and a solvent run was performed with acetone to confirm the performance under the required operating pressures (6–8 bar). A process flow diagram is provided in Figure 3, and a summary of the reaction conditions utilized for this specific demonstration run, as detailed in the previous sections, is provided in Table 3. The system was operated for 51 consecutive hours to deliver a 91% solution assay yield, corresponding to a productivity of 26.9 g of crude product/h (646 g/day). As detailed in Figure 4,
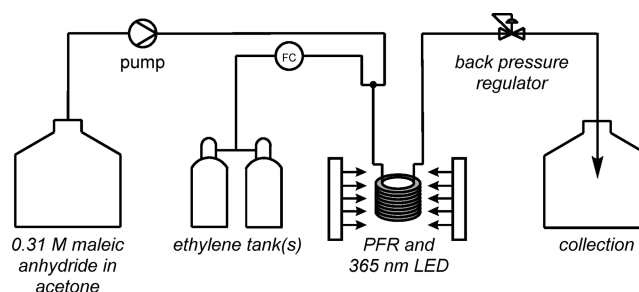
Figure 3. Process flow diagram for the 500 g/day demonstration run.

Table 3. Experimental Conditions for the Demonstration Run

parameter	target
maleic anhydride concentration	0.31 M
photosensitizer loading	10 mol %
solvent	acetone
temperature	ambient
pressure	6–8 bar
residence time	120 min
irradiation volume	1.56 L
tubing material	FEP
tubing outer diameter	10 mm

samples were collected at the outlet of the reactor at 4 h intervals and analyzed by GC and qNMR for conversion and assay yield, respectively. The slight variability observed for the maleic anhydride concentration over the 51 h run was attributed to the use of a manual control valve for ethylene flow. An automated mass-flow controller was implemented in subsequent runs to minimize the impact of flow rate drift.

Development of an Isolation Protocol. Attention turned to the development of a robust isolation protocol using bulk crude material from the successful proof-of-concept run. A preliminary screen of crystallization solvents identified methyl *tert*-butyl ether (MTBE) and cyclohexane as potential candidates for use as antisolvents. A comprehensive evaluation is provided in the Supporting Information. The high dilution of the photochemical process (33 volumes), coupled with the high solubility of cyclobutane **2** in acetone (>100 mg/mL), rendered the direct addition of cyclohexane or MTBE as an antisolvent impractical. Distillation followed by solvent exchange to the crystallization solvent delivered significantly improved recovery but inconsistent purity profiles. The

Table 2. Impact of Equipment Design on the Reaction Productivity

entry[a]	tubing o.d. (mm)[b]	benzophenone loading (mol %)	residence time (min)[c]	mixer type	LED panels (input power)[d]	maleic anhydride (GC area %)	reaction productivity (g/h)[e]
1	6	10	120	union tee	2 × 300 W (100%)	<5	17.1
2	10	10	120	union tee	2 × 300 W (100%)	<5	19.5
3	10	10	90	union tee	2 × 300 W (100%)	5–10	19.4
4	10	10	90	mixing tank	2 × 300 W (100%)	4–7	22.6
5	6	20	90	union tee	3 × 300 W (100%)	5	24.5
6	6	20	90	union tee	3 × 300 W (80%)	15	18.6
7	6	20	90	union tee	3 × 300 W (40%)	42	11.9

[a]A 0.31 M solution of maleic anhydride in acetone was combined with ethylene at 7 bar and passed through a 1.0–1.3 L irradiation zone. [b]1 mm wall thickness. [c]Based on the volumetric flow rate of the maleic anhydride feed stream. [d]A 30 cm × 40 cm panel of 365 nm surface-mounted LEDs with an irradiation intensity of 60 mW/cm^2 at the tubing was used. [e]As determined by qNMR analysis of the crude reaction stream in deuterated acetone using 1,3,5-trimethoxybenzene as the standard.
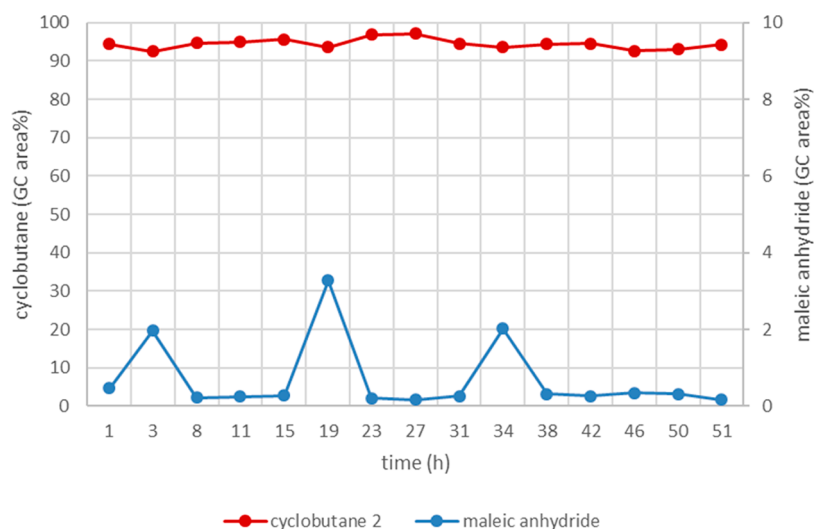
Figure 4. Sampling results for the 51 h demonstration run.

potency of crystalline solids by qNMR was in the range of 90−95 wt % despite high purity by GC area %. During this evaluation, a poorly soluble white precipitate was collected that could not be readily characterized by ^{1}H NMR or GC analysis; this material, which is suspected to be a polymeric product of maleic anhydride and ethylene,[4a] accounts for the low potency of the isolated solids.

Additional studies were conducted to optimize the crystallization conditions such that the polymeric impurity could be rejected prior to the final isolation of cyclobutane 2 as a high-potency crystalline solid. Of the solvents evaluated, toluene demonstrated high solubility for cyclobutane 2 and poor solubility for the impurity; therefore, a procedure was designed such that dissolution of cyclobutane 2 could be achieved in toluene (1 L/kg) and MTBE (2.5 L/kg) at elevated temperature (55 °C), followed by a filtration operation to purge the undesired impurity and limit losses of the desired product to 2−3%. The filtrate could be cooled to generate a slurry and filtered to isolate cyclobutane 2 as a white crystalline solid with 80% recovery from the crude mixture and 73% overall isolated yield (Figure 5).
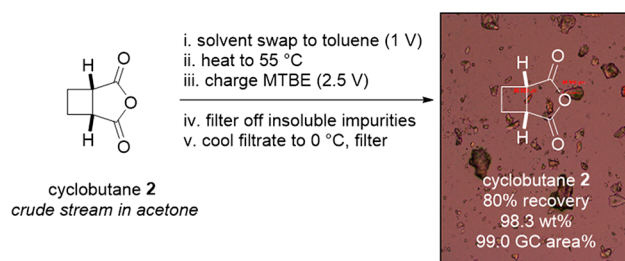

Figure 5. Isolation protocol for cyclobutane 2 and representative polarized-light microscope image of the crystalline solid.

Equipment Design and Build for the Execution of a 5 kg/day Pilot. Upon successful completion of the optimization and demonstration phases of the program, the team launched an effort to design, build, and implement a skid capable of delivering the target compound at 5 kg/day. A process hazard analysis (PHA) was conducted to inform the design of the high-throughput skid and ensure safe implementation in the production setting. Elements of the PHA and associated design modifications are listed below and illustrated in Figure 6:

- Temperature control and alarms: A programmable logic controller (PLC) continuously monitors the temperature of the process (T1) and LED lamp banks. An alarm is set to alert operators of any deviation.
- Dilution of excess ethylene below the lower explosion limit (LEL): A vapor/liquid separator is introduced at the outlet of the reaction and continuously purged with nitrogen to ensure that excess ethylene is diluted below its LEL. Visual inspection of the nitrogen flow is performed at regular intervals.
- Location of ethylene feed tanks: The feed tanks are relocated to a demarcated space equipped with a manifold to alternate between tanks without disruption to the process.
- Inclusion of LEL sensors: LEL sensors are installed in all rooms and confined spaces where ethylene could accumulate. The LEL sensor located inside the photoreactor enclosure is interlocked to immediately stop the flow of both the ethylene and acetone solutions.
- Inclusion of a pressure sensor: The PLC continuously monitors the system pressure via the P1 transmitter. This sensor is interlocked to stop the flow of both the ethylene and acetone solutions in the event of pressure increase (e.g., clog) or pressure decrease (e.g., broken line).

The production skid, including the safety considerations detailed above, comprised three separate modules in series of FEP tubing (20.76 L irradiated volume, 10 mm o.d.) and 6 × 3 kW 365 nm LED panels (Figure 7). A one-third scale-down run was performed over 24 h using a single module prior to completing the assembly (Figure 8). The system demonstrated higher variability than had been observed in previous runs; however, it provided insightful information for assembly of the full-scale skid. The fluctuations in conversion were attributed in part to a faulty back-pressure regulator (BPR), which impacted the ethylene stoichiometry and mean residence time. Furthermore, the solution temperature within the reaction module reached 52 °C due to the significant heat generated from the LED bank. For future runs, this was addressed by adjusting the flow rate of the cooling medium, relocating the
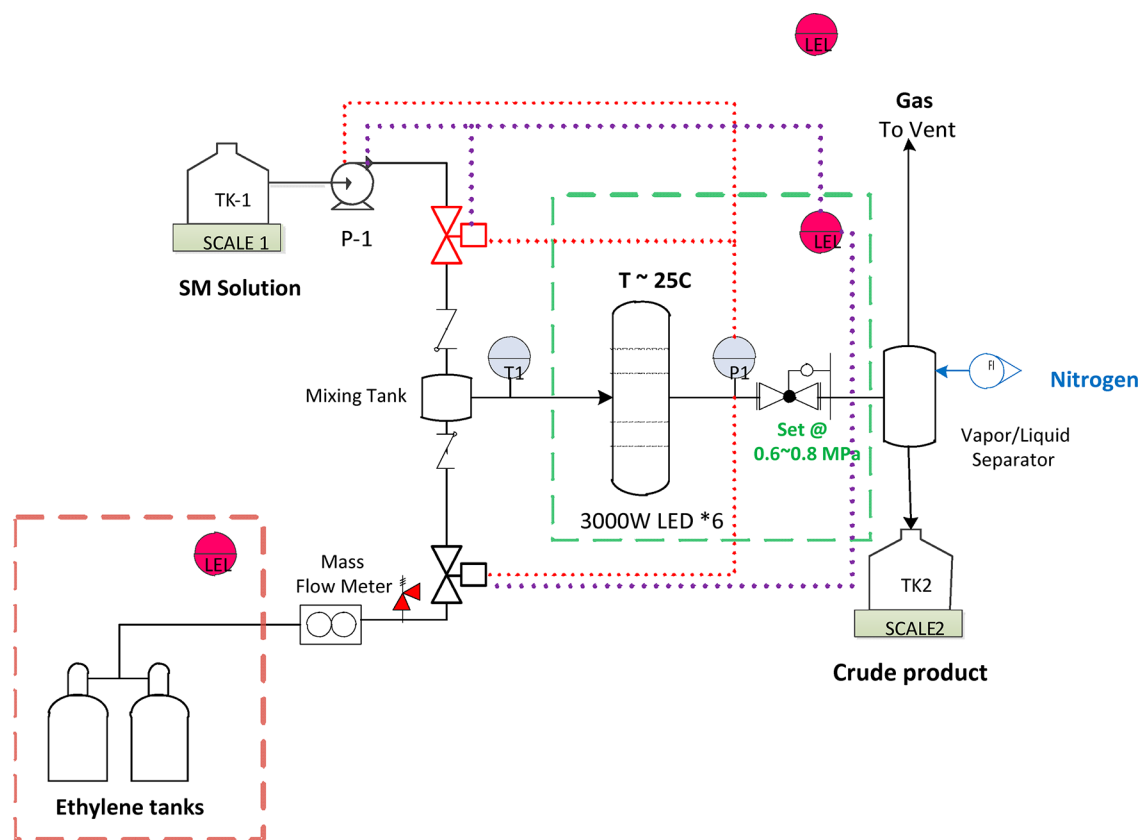
Figure 6. Modifications to the skid to support safe implementation in the production setting.
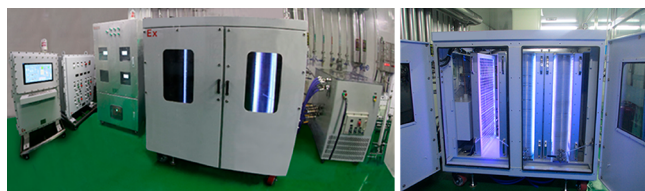

Figure 7. Pictures of the production-scale photochemical skid.

thermocouple to improve accuracy, and including a convection fan within the module. Cyclobutane **2** was isolated in 58% yield with 97.2% potency and 99.3 purity by GC area %, providing assurance that the isolation procedure could reject unreacted starting material in the event of incomplete conversion.

The information learned from the pilot run was incorporated into the full-scale production skid, and an engineering run was
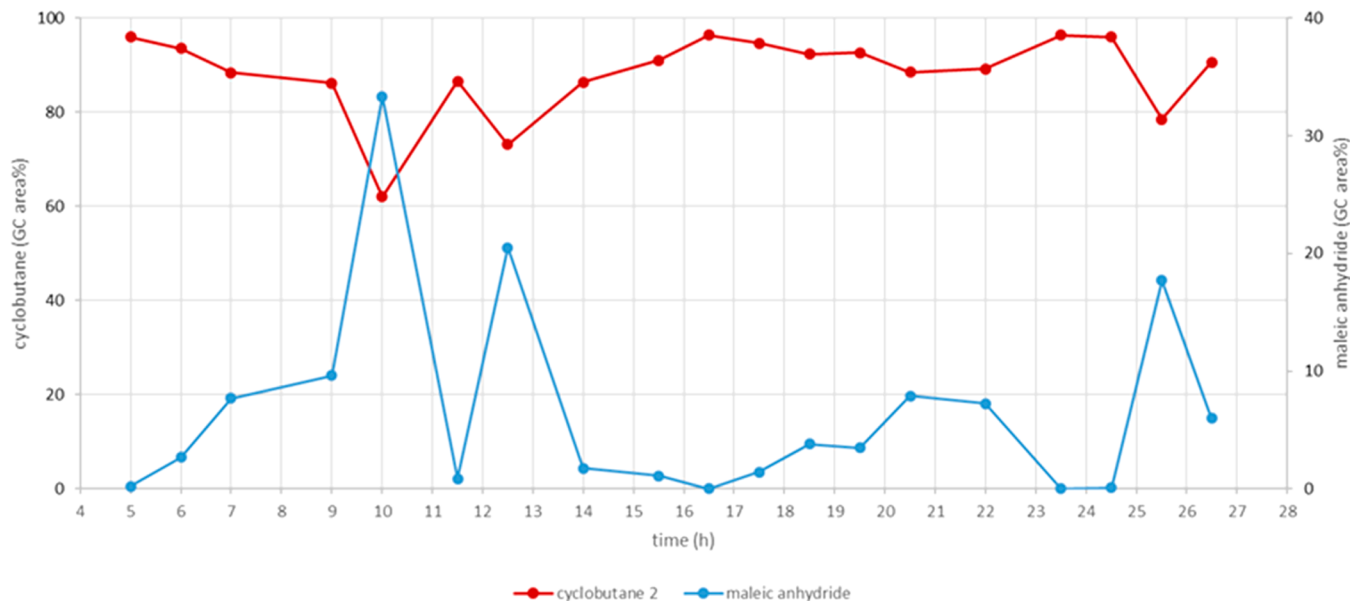

Figure 8. Summary of the 24 h pilot run performed at one-third production scale.
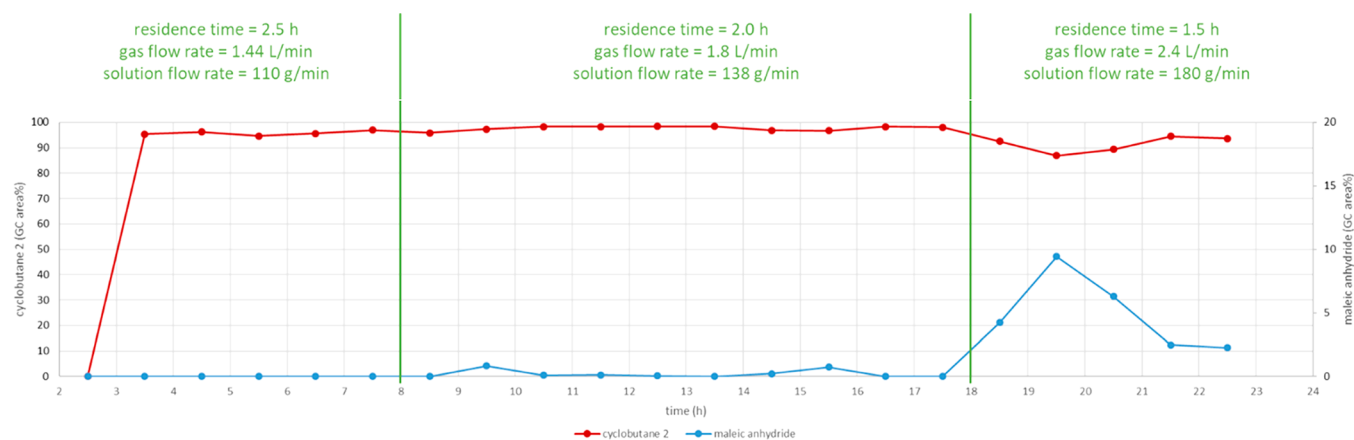
Figure 9. Summary of the full-scale engineering run.

Table 4. Experimental Conditions for the Demonstration Runs

run	batch	residence time (h)	mass of isolated **2** (yield)	potency (wt %)	purity (GC area %)
engineering (24 h)	1	2.5	1.05 kg (65%)	98	99.0
	2	2.0	2.85 kg (64%)	97	98.9
	3	1.5	0.98 kg (63%)	97	98.4
commissioning (45 h)	1	2.0[a]	9.87 kg (64%)	98	98.0

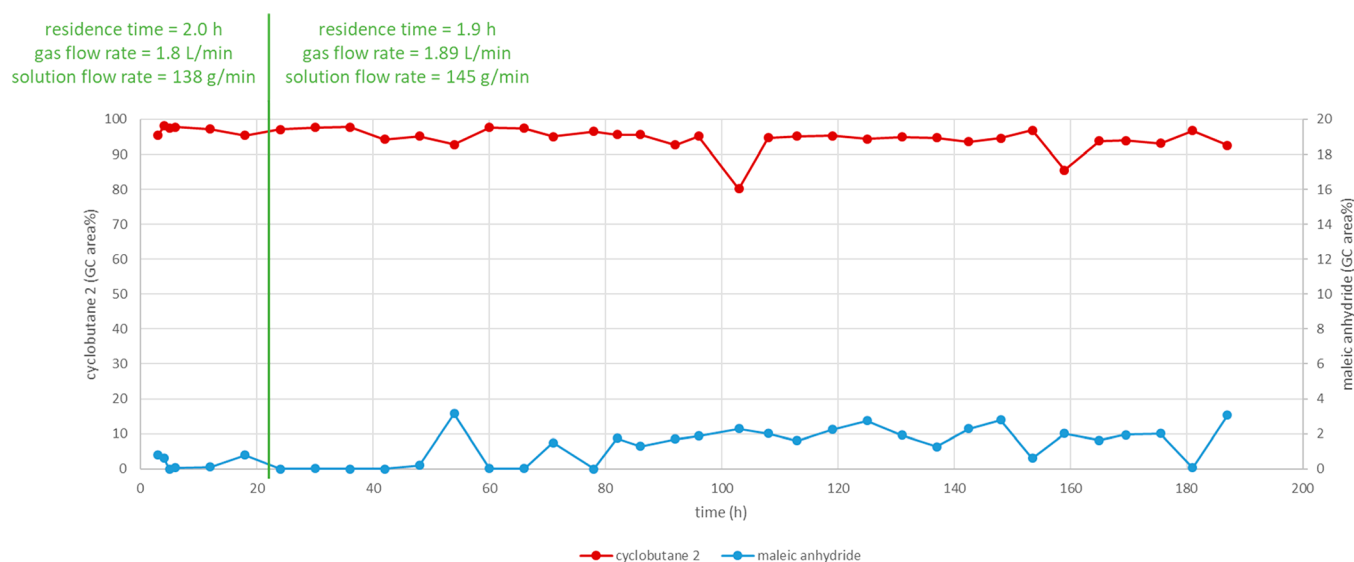[a] The system was initiated for 5 h at a residence time of 1.72 h.

Figure 10. Results of a production batch to prepare cyclobutane **2**.

performed to verify the process performance. Three conditions were evaluated during this run to assess the limits of the system and generate an operational envelope; specifically, the residence time was varied between 1.5 and 2.5 h through adjustment of the solution and gas flow rates. When a state of control was reached, the conversion target (<5 GC area % maleic anhydride) was achieved and maintained for both 2.0 and 2.5 h residence times (Figure 9). Decreasing the residence time to 1.5 h resulted in increased levels of unreacted starting material. The average temperature and pressure readings for the duration of the full-scale engineering run were 40 °C and 7 bar, respectively. A final commissioning batch was run under the optimal conditions for an uninterrupted period of 45 h. Table 4 provides a summary of these runs, including the results

of the crystallization procedure to isolate cyclobutane **2** in high purity from the crude reaction stream.

Multiple production batches were executed using the optimized conditions to generate >250 kg of cyclobutane **2** meeting the requisite purity targets. The in-process results of a single production batch, performed uninterrupted for a period of 1 week, are illustrated in Figure 10. The residence time was decreased from 2.0 to 1.9 h for a minor improvement in overall productivity without impact on the material quality. The conversion was assessed every 6 h to ensure that a state of control had been achieved and was maintained; the target of <5 GC area % maleic anhydride was met at every sampling point. Fouling was observed on the interior of the FEP tubing and back-pressure regulator upon completion of the run and inspection of the system. Cleaning and replacement protocols

were instituted between production runs as a measure to ensure adequate light penetration and to avoid clogging of the lines. A total of 51.8 kg of cyclobutane **2** of 97.9 wt % and 100.0 purity by GC area % was delivered from this specific campaign, exceeding the 5 kg/day production target.

CONCLUSIONS

The continuous [2 + 2] photocycloaddition of maleic anhydride and ethylene was performed on multikilogram scale to provide cyclobutane **2** as a white crystalline solid at throughputs exceeding 5 kg/day. Key to this effort was focused reaction optimization, execution of demonstration runs utilizing equipment representative of the production skid, comprehensive studies focused on isolation of the crystalline solid from the crude reaction stream, and an exhaustive evaluation of process safety prior to production.

EXPERIMENTAL SECTION

General Procedure for Reaction Optimization. To a 500 mL volumetric flask were charged maleic anhydride (12.25 g, 125 mmol), benzophenone (2.28 g, 12.5 mmol), and acetone (ca. 485 mL) to a total volume of 500 mL. The solution was sparged with nitrogen gas for 20 min and then continuously with ethylene at ambient pressure. The solution was recirculated at 80 mL/min through 0.31 L of FEP tubing (o.d. = 3 mm, i.d. = 2 mm, irradiation volume = 0.25 L), wrapped around four 40 W 365 nm LED arrays (irradiation intensity = 10 mW/cm^2) and back into the 500 mL flask until <5−10 GC area % maleic anhydride remained. The crude reaction mixture was concentrated in vacuo and slurried with cyclohexane (2 mL/g) at 20 °C for 30 min followed by filtration. The cake was reslurried with MTBE (1 mL/g) at 20 °C for 30 min, filtered, and washed with MTBE (0.5 mL/g) to afford cyclobutane **2** as a crystalline solid.

Procedure for the 500 g/day Demonstration. To a 50 L flask were charged maleic anhydride (1.19 kg, 12.1 mol), benzophenone (0.220 kg, 1.21 mol), and acetone (39.0 L, 32.8 L/kg). The solution was sparged with nitrogen gas for 20 min prior to use. The solution was pumped at 10.4 g/min, mixed with ethylene (136 mL/min) via a tee mixer, and then pumped through a 1.56 L coil of FEP tubing (o.d. = 10 mm, i.d. = 8 mm) wrapped around three 300 W panels of 365 nm LEDs (dimensions: 30 cm × 40 cm; irradiation intensity = 60 mW/cm^2) at a system pressure of 6−8 bar. Samples of the reaction stream were collected at regular intervals for analysis by GC, and the bulk solution was collected into a 50 L flask. The reaction mixture was concentrated in vacuo to provide crude cyclobutane **2** in 91% potency-adjusted yield, corresponding to a productivity of 26.9 g/h. The material from this demonstration run was segregated and used for the development of the isolation strategy; therefore, a cumulative isolated yield is not available.

Representative Production-Scale Procedure. To a 3000 L stainless steel reactor were added acetone (2180 L, 33.0 L/kg), maleic anhydride (66.0 kg, 673 mol), and benzophenone (12.3 kg, 67.5 mol). Acetone was pumped through a 29 L FEP coil with an effective irradiation volume of 21 L (o.d. = 10 mm, i.d. = 8 mm) until the coil was full, and then the system was pressurized to 6−8 bar with ethylene gas flow and equilibrated for 30 min. The 365 nm LEDs were turned on (six 3 kW surface-mounted panels; irradiation intensity = 60 mW/cm^2), and the maleic anhydride solution

and ethylene gas feeds were initiated at 138.4 g/min and 1800 mL/min (1.5 equiv), respectively. Samples of the reaction stream were collected at regular intervals for analysis by GC, and the bulk solution was collected into a 2000 L stainless steel reactor. The crude mixture was concentrated until the residual of acetone was 45 wt %, and then the solvent was exchanged with toluene (197 L, 3.0 L/kg) until the acetone content was <1 wt % and the toluene content was around 25−40 wt %. The solution was warmed to 60 °C, and MTBE (132 L, 2.0 L/kg) was added. The resultant slurry was agitated for 2 h at 60 °C and filtered to remove an insoluble impurity. The supernatant containing cyclobutane **2** was collected in a 500 L stainless steel reactor and cooled to 0 °C at a rate of 5−10 °C/h. The slurry was filtered and washed two times with MTBE (66 L, 1.0 L/kg). The filter cake was dried under a nitrogen flow at 30−50 °C to afford 51.8 kg (61% yield) of cyclobutane **2** as a white crystalline solid with 97.9% potency, 100.0 purity by GC area %, and spectra matching those previously reported:[6] ^{1}H NMR (400 MHz, CD$_3$COCD$_3$) δ 3.51−3.54 (m, 2H), 2.68−2.69 (m, 2H), 2.24−2.28 (m, 2H); melting point = 72−76 °C.

ASSOCIATED CONTENT

SI   **Supporting Information**

The Supporting Information is available free of charge at https://pubs.acs.org/doi/10.1021/acs.oprd.0c00185.

Details of analytical methods and experimental results (PDF)

AUTHOR INFORMATION

Corresponding Authors

Matthew G. Beaver − *Process Development, Amgen, Inc., Cambridge, Massachusetts 02142, United States;* ⊙ orcid.org/0000-0003-3816-4601; Email: mbeaver@amgen.com

En-xuan Zhang − *Asymchem Life Science (Tianjin) Co., Ltd., Tianjin 300457, China;* Email: zhangenxuan@asymchem.com.cn

Authors

Zhi-qing Liu − *Asymchem Life Science (Tianjin) Co., Ltd., Tianjin 300457, China*

Song-yuan Zheng − *Asymchem Life Science (Tianjin) Co., Ltd., Tianjin 300457, China*

Bin Wang − *Asymchem Life Science (Tianjin) Co., Ltd., Tianjin 300457, China*

Jiang-ping Lu − *Asymchem Life Science (Tianjin) Co., Ltd., Tianjin 300457, China*

Jian Tao − *Asymchem Life Science (Tianjin) Co., Ltd., Tianjin 300457, China*

Miguel Gonzalez − *Asymchem Life Science (Tianjin) Co., Ltd., Tianjin 300457, China*

Siân Jones − *Process Development, Amgen, Inc., Thousand Oaks, California 91320, United States*

Jason S. Tedrow − *Process Development, Amgen, Inc., Cambridge, Massachusetts 02142, United States;* ⊙ orcid.org/0000-0002-5663-2360

Complete contact information is available at:
https://pubs.acs.org/10.1021/acs.oprd.0c00185

Notes

The authors declare no competing financial interest.

■ ACKNOWLEDGMENTS

■ REFERENCES

(1) For reviews, see: (a) Poplata, S.; Tröster, A.; Zou, Y.-Q.; Bach, T. Recent Advances in the Synthesis of Cyclobutanes by Olefin [2 + 2] Photocycloaddition Reactions. *Chem. Rev.* **2016**, *116*, 9748−9815. (b) Romero, N. A.; Nicewicz, D. A. Organic Photoredox Catalysis. *Chem. Rev.* **2016**, *116*, 10075−10166. (c) Douglas, J. J.; Sevrin, M. J.; Stephenson, C. R. J. Visible Light Photocatalysis: Applications and New Disconnections in the Synthesis of Pharmaceutical Agents. *Org. Process Res. Dev.* **2016**, *20*, 1134−1147. (d) Teegardin, K.; Day, J. I.; Chan, J.; Weaver, J. Advances in Photocatalysis: A Microreview of Visible Light Mediated Ruthenium and Iridium Catalyzed Organic Transformations. *Org. Process Res. Dev.* **2016**, *20*, 1156−1163. (e) Skubi, K. L.; Blum, T. R.; Yoon, T. P. Dual Catalysis Strategies in Photochemical Synthesis. *Chem. Rev.* **2016**, *116*, 10035−10074. (f) Zhou, Q.-Q.; Zou, Y.-Q.; Lu, L.-Q.; Xiao, W.-J. Visible-Light-Induced Organic Photochemical Reactions through Energy-Transfer Pathways. *Angew. Chem., Int. Ed.* **2019**, *58*, 1586−1604. (g) McAtee, R. C.; McClain, E. J.; Stephenson, C. R. J. *Trends in Chemistry* **2019**, *1*, 111−125.

(2) Beatty, J. W.; Douglas, J. J.; Miller, R.; McAtee, R. C.; Cole, K. P.; Stephenson, C. R. J. Photchemical Perfluoroalkylation with Pyridine *N*-Oxides: Mechanistic Insights and Performance on a Kilogram Scale. *Chem.* **2016**, *1*, 456−472.

(3) Harper, K. C.; Moschetta, E. G.; Bordawekar, S. V.; Wittenberger, S. J. A Laser Driven Flow Chemistry Platform for Scaling Photochemical Reactions with Visible Light. *ACS Cent. Sci.* **2019**, *5*, 109−115.

(4) For recent reviews detailing the implementation of continuous processing for photochemical processes, see: (a) Knowles, J. P.; Elliott, L. D.; Booker-Milburn, K. I. Flow Photochemistry: Old Light through New Windows. *Beilstein J. Org. Chem.* **2012**, *8*, 2025−2052. (b) Schuster, E. M.; Wipf, P. Photochemical Flow Reactions. *Isr. J. Chem.* **2014**, *54*, 361−370. (c) Su, Y.; Straathof, N. J.; Hessel, V.; Noël, T. Photochemical Transformations Accelerated in Continuous-Flow Reactors: Basic Concepts and Applications. *Chem. - Eur. J.* **2014**, *20*, 10562−10589. (d) Cambié, D.; Bottecchia, C.; Straathof, N. J.; Hessel, V.; Noël, T. Applications of Continuous-Flow Photochemistry in Organic Synthesis, Material Science, and Water Treatment. *Chem. Rev.* **2016**, *116*, 10276−10341. (e) Loubiére, K.; Oelgemöller, M.; Aillet, T.; Dechy-Cabaret, O.; Prat, L. Continuous-Flow Photochemistry: A Need for Chemical Engineering. *Chem. Eng. Process.* **2016**, *104*, 120−132. (f) Politano, F.; Oksdath-Mansilla, G. Light on the Horizon: Current Research and Future Perspectives in Flow Photochemistry. *Org. Process Res. Dev.* **2018**, *22*, 1045−1062. (g) Sambiagio, C.; Noël, T. Flow Photochemistry: Shine Some Light on Those Tubes. *Trends Chem.* **2020**, *2*, 92−106.

(5) For representative examples of this approach to cyclobutane **2** at lab scale (grams) using medium-pressure mercury lamps, see: (a) Owsley, D. C.; Bloomfield, J. J. Photochemical [2 + 2] Cycloaddition Reactions at Low Temperatures. Synthesis of Bridgehead Substituted Bicyclo[n.2.0] dicarboxylates from Maleic Acid Derivatives and Ethylene. *J. Org. Chem.* **1971**, *36*, 3768−3772. (b) Gu, X.; Xian, M.; Roy-Faure, S.; Bolte, J.; Aitken, D. J.; Gefflaut, T. Synthesis of the Constrained Glutamate analogues (2*S*,1′*R*,2′*R*)- and (2*S*,1′*S*,2′*S*)-2-(2′-carboxycyclobutyl)glycines L-CBG-II and L-CBG-I by Enzymatic Transamination. *Tetrahedron Lett.* **2006**, *47*, 193−196. (c) Faure, S.; Jensen, A. A.; Maurat, V.; Gu, X.; Sagot, E.; Aitken, D. J.; Bolte, J.; Gefflaut, T.; Bunch, L. Stereoselective Chemoenzymatic Synthesis of the Four Stereoisomers of L-2-(2-carboxycyclobutyl)glycine and Pharmacological Characterization at

Human Excitatory Amino Acid Transporter Subtypes 1, 2, and 3. *J. Med. Chem.* **2006**, *49*, 6532−6538. (d) Mercer, J. A. M; Cohen, C. M.; Shuken, S. R.; Wagner, A. M.; Smith, M. W.; Moss, R. F., III; Smith, M. D.; Vahala, R.; Gonzalez-Martinez, A.; Boxer, S. G.; Burns, N. Z. Chemical Synthesis and Self-Assembly of Ladderane Phospholipid. *J. Am. Chem. Soc.* **2016**, *138*, 15845−15848.

(6) Corcoran, E. B.; Levesque, F.; McMullen, J. P.; Naber, J. R. Studies Toward the Scaling of Gas−Liquid Photocycloadditions. *Chem. Photo. Chem.* **2018**, *2*, 931−937.

(7) Williams, J. D.; Nakano, M.; Gérardy, R.; Rincón, J. A.; de Frutos, Ó.; Mateos, C.; Monbaliu, J. C. M.; Kappe, C. O. Finding the perfect match: A combined computational and Experimental Study toward efficient and Scalable Photosensitized [2 + 2] cycloaddition in flow. *Org. Process Res. Dev.* **2019**, *23*, 78−87.

(8) (a) Elliott, L. D.; Berry, M.; Harji, B.; Klauber, D.; Leonard, J.; Booker-Milburn, K. I. A Small-Footprint, High Capacity Flow Reactor for UV Photochemical Synthesis on the Kilogram Scale. *Org. Process Res. Dev.* **2016**, *20*, 1806−1811. (b) Cox, B.; Booker-Milburn, K. I.; Elliott, L. D.; Robertson-Ralph, M.; Zdorichenko, V. Escaping from Flatland: [2 + 2] Photocycloaddition; Conformationally Constrained sp^3-rich Scaffolds for Lead Generation. *ACS Med. Chem. Lett.* **2019**, *10*, 1512−1517.

(9) Solution concentrations ranging from 0.1 to 0.5 M were suitable to maximize the productivity and minimize the formation of dimer **4** observed at higher concentrations.

(10) FEP was chosen as the tubing material because of its low cost, ease of replacement, chemical compatibility, pressure rating, and light-transmission properties. For example, see: Hook, B. D. A.; Dohle, W.; Hirst, P. R.; Pickworth, M.; Berry, M. B.; Booker-Milburn, K. I. A Practical Flow Reactor for Continuous Organic Photochemistry. *J. Org. Chem.* **2005**, *70*, 7558−7564.

(11) Additional details are available in the Experimental Section.

(12) Horie, T.; Sumino, M.; Tanaka, T.; Matsushita, Y.; Ichimura, T.; Yoshida, J. Photodimerization of Maleic Anhydride in a Microreactor Without Clogging. *Org. Process Res. Dev.* **2010**, *14*, 405−410.

(13) The Paternó−Büchi adduct of acetone and maleic anhydride, the major product formed upon irradiation with a medium-pressure Hg lamp, was not observed under these conditions. See: Turro, N. J.; Wriede, P. A. Photocycloadditions of some alkyl ketones to 1,2-dicyanoethylene maleic anhydride and 1-methoxy-1-butene. *J. Org. Chem.* **1969**, *34*, 3562−3565.

(14) Sahgal, A.; La, H. M.; Hayduk, W. Solubility of Ethylene in Several Polar and non-Polar Solvents. *Can. J. Chem. Eng.* **1978**, *56*, 354−357.

(15) Metrics for product quality and yield were assessed using a first-generation isolation protocol detailed in the Experimental Section. For reference, a 5 mol % loading of benzophenone provided a white crystalline solid in 71% yield with 95.9 wt % potency, whereas a 20 mol % loading generated a yellow solid in 74% yield with 91.5 wt % potency.